Electronic Supplementary Material (ESI) for CrystEngComm.

Influence of organic cations on π-stacking of semiquinone radical anions

Supplement

Krešimir Molčanov*[a], Valentina Milašinović[a], Nives Ivić[a], Vladimir Stilinović[b], Dinko Kolarić[c], Biserka Kojić-Prodić[a]

[a] Rudjer Bošković Institute, Bijenička 54, Zagreb HR-10000, Croatia

[b] Department of Chemistry, Faculty of Science, University of Zagreb, Horvatovac 102a, Zagreb HR-10000, Croatia

[c] Special Hospital for Medical Rehabilitation, Daruvarske Toplice, Julijev park 1, Daruvar HR-43500, Croatia

e-mail: kmolcano@irb.hr

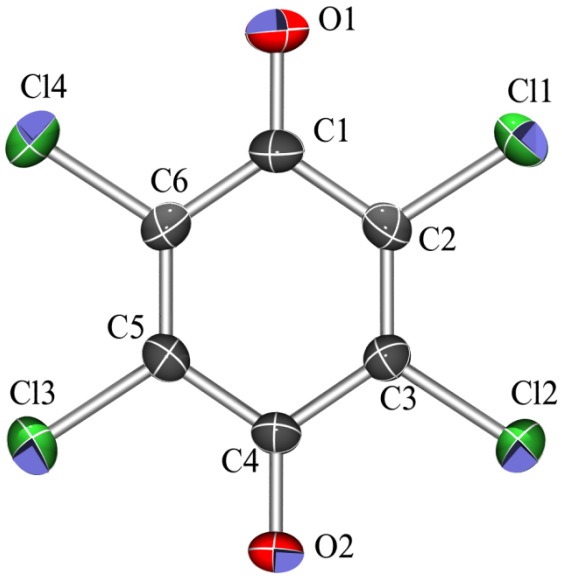

Figure S1 ORTEP-3 drawing of Cl_4Q radical anion in **1**·Cl_4Q. Displacement ellipsoids are drawn for the probability of 50 %.

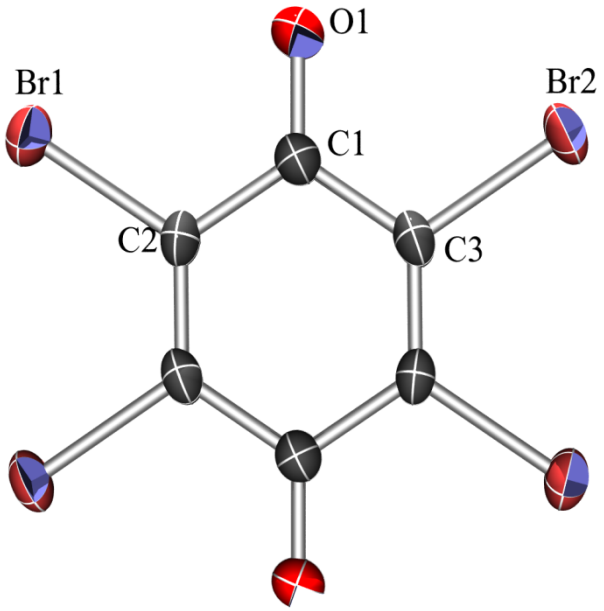

Figure S2 ORTEP-3 drawing of Br_4Q radical anion in **1**·Br_4Q. Displacement ellipsoids are drawn for the probability of 50 %.

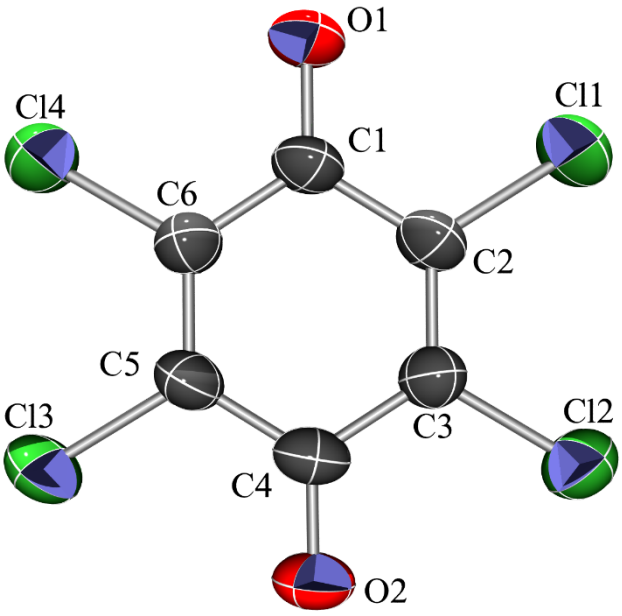

Figure S3 ORTEP-3 drawing of Cl_4Q radical anion in **2**·Cl_4Q. Displacement ellipsoids are drawn for the probability of 50 %.

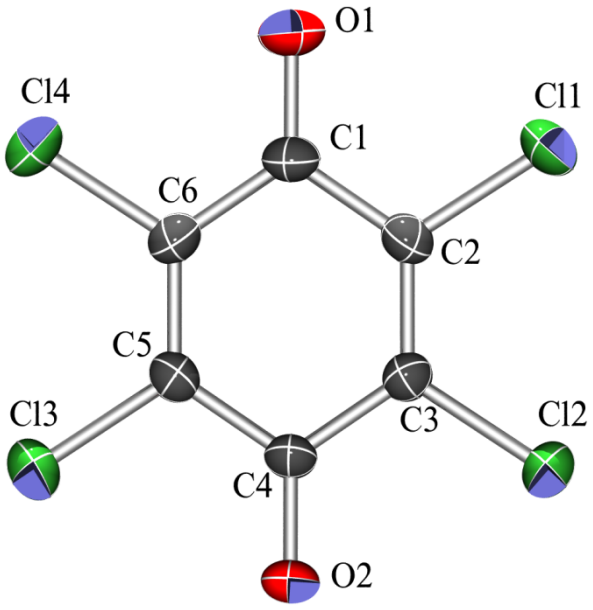

Figure S4 ORTEP-3 drawing of Cl_4Q radical anion in **3**·Cl_4Q. Displacement ellipsoids are drawn for the probability of 50 %.

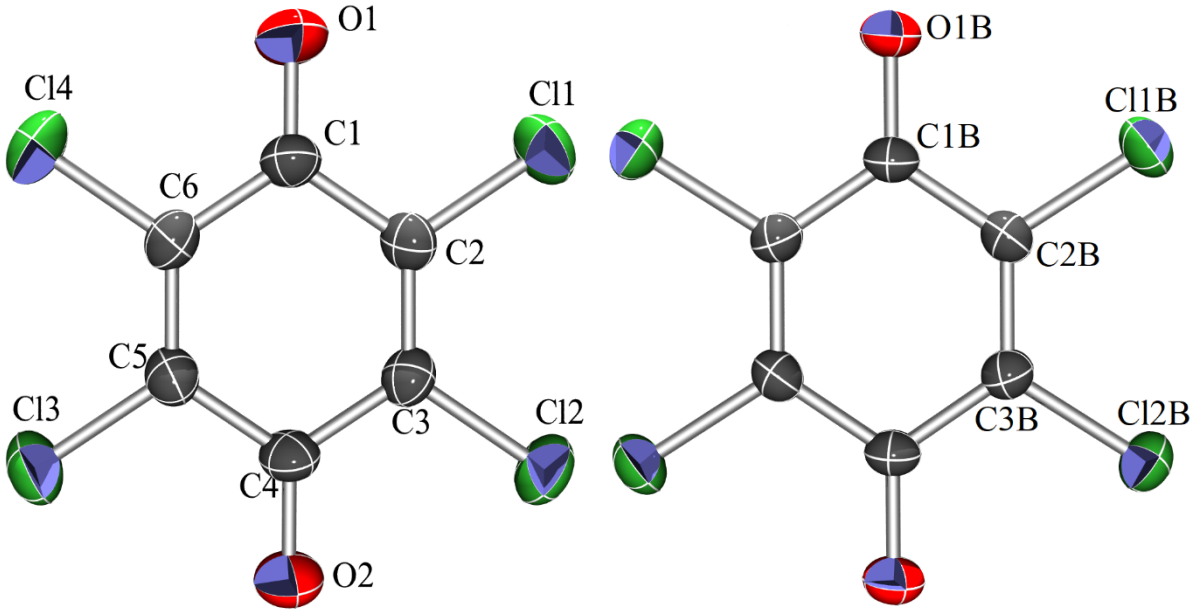

Figure S5 ORTEP-3 drawings of two symmetry-inequivalent partially charged Cl_4Q radicals in $\mathbf{4}_2{\cdot}(Cl_4Q)_3$. Displacement ellipsoids are drawn for the probability of 50 %.

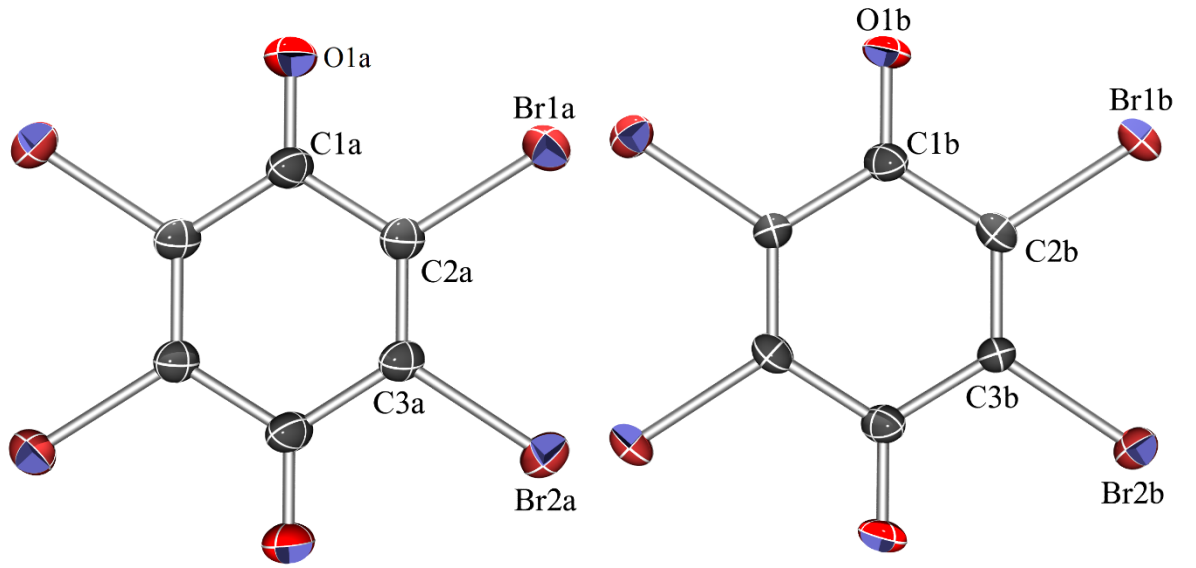

Figure S6 ORTEP-3 drawings of two symmetry-independent Br_4Q radical anions (A and B, respectively) in $\mathbf{4}_2{\cdot}(Br_4Q)_2$. Displacement ellipsoids are drawn for the probability of 50 %.

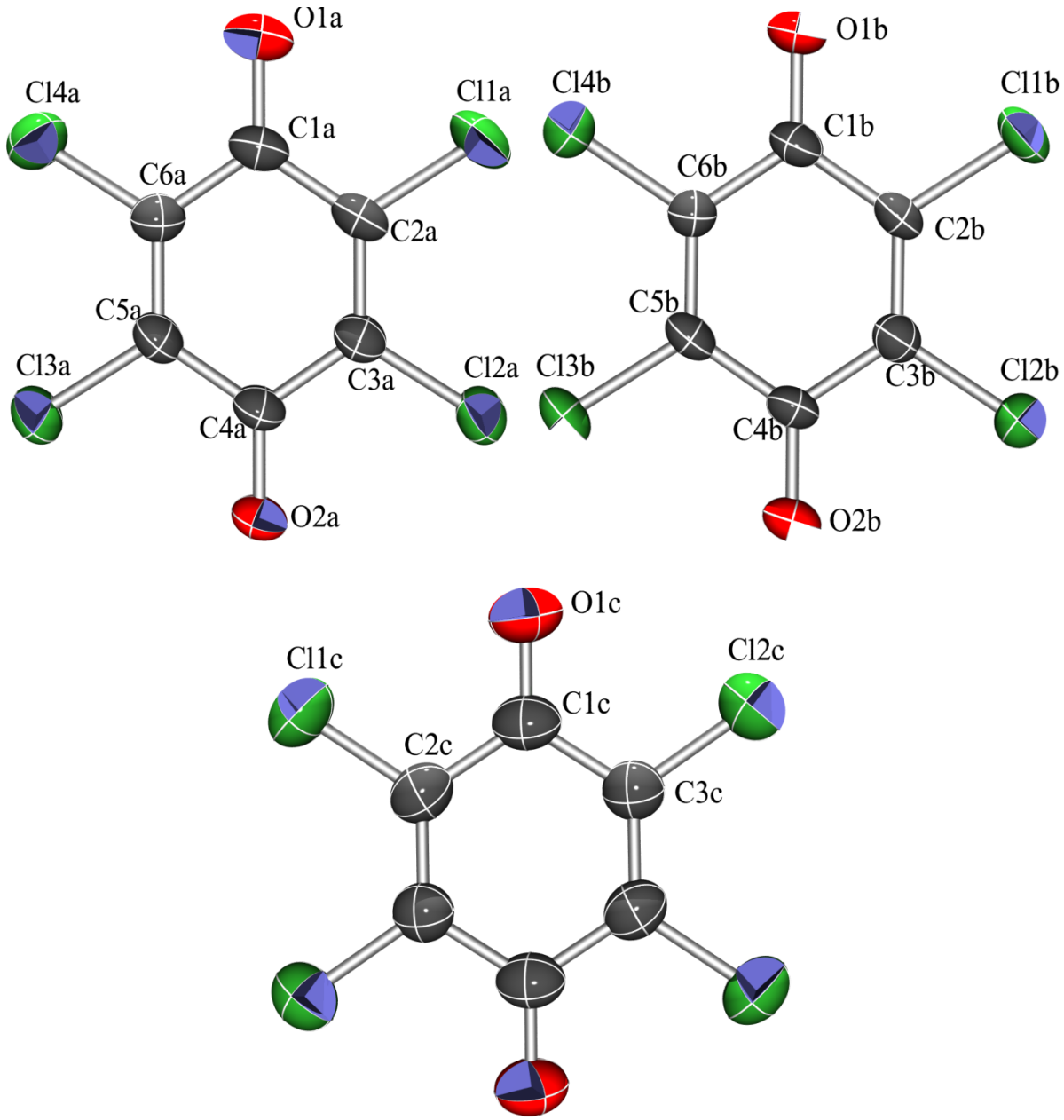

Figure S7 ORTEP-3 drawings of a) and b) two symmetry-independent Cl_4Q radical anions and c) neutral molecule of Cl_4Q in $\mathbf{5}_4 \cdot (Cl_4Q)_5$. Displacement ellipsoids are drawn for the probability of 50 %.

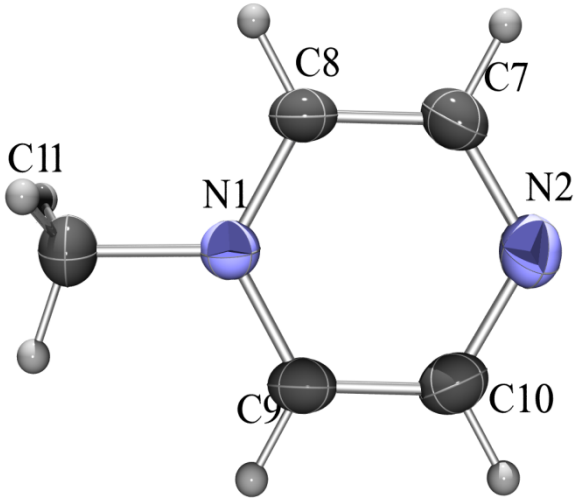

Figure S8 ORTEP-3 drawing of *N*-methylpyrazinium cation in **1**·Cl_4Q. Displacement ellipsoids are drawn for the probability of 50 % and hydrogen atoms are shown as spheres of arbitrary radii.

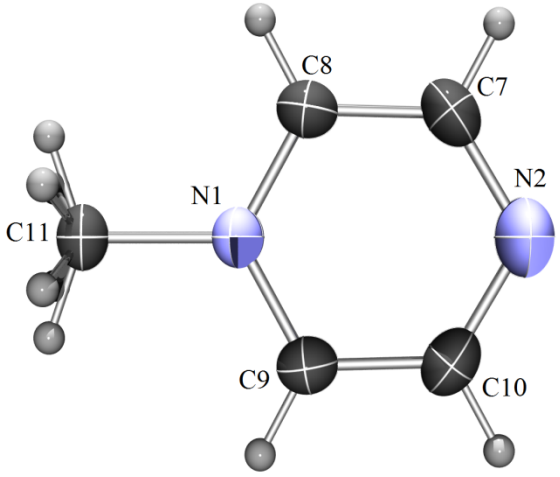

Figure S9 ORTEP-3 drawing of *N*-methylpyrazinium cation in **1**·Br_4Q. Displacement ellipsoids are drawn for the probability of 50 % and hydrogen atoms are shown as spheres of arbitrary radii.

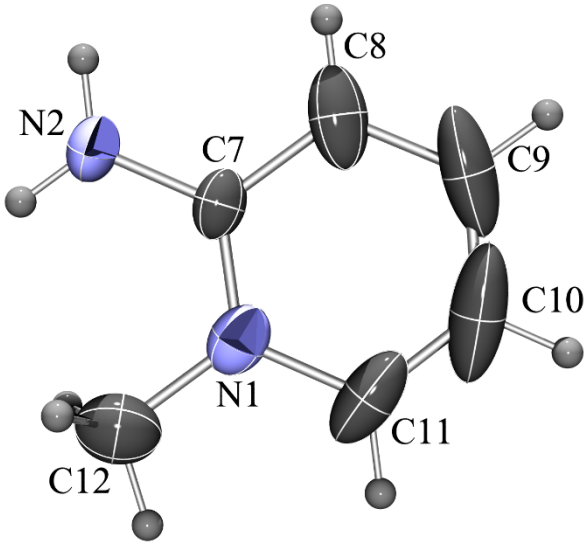

Figure S10 ORTEP-3 drawing of *N*-methyl-2-aminopyridinium cation in **2**·Cl_4Q. Displacement ellipsoids are drawn for the probability of 50 % and hydrogen atoms are shown as spheres of arbitrary radii.

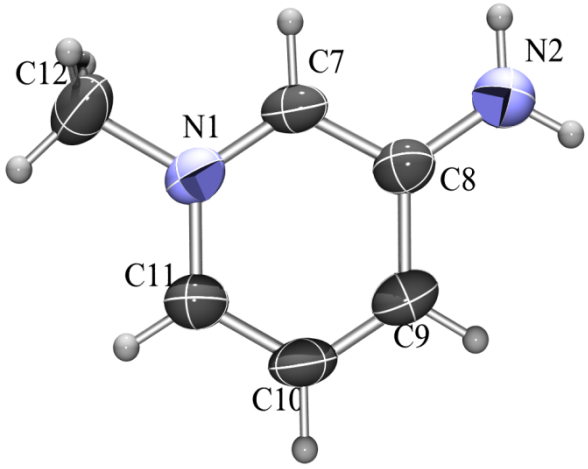

Figure S11 ORTEP-3 drawing of *N*-methyl-3-aminopyridinium cation in **3**·Cl_4Q. Displacement ellipsoids are drawn for the probability of 50 % and hydrogen atoms are shown as spheres of arbitrary radii.

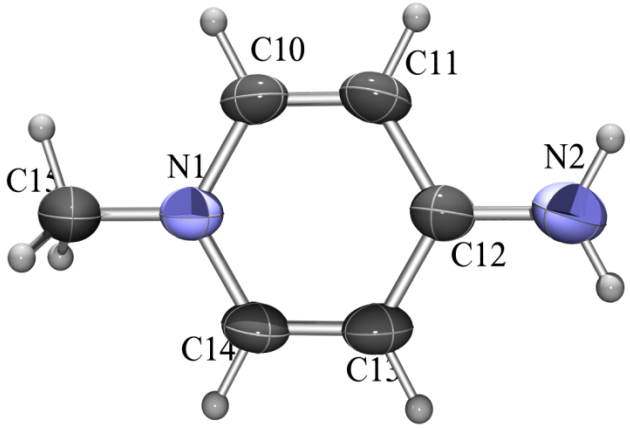

Figure S12 ORTEP-3 drawing of a disordered *N*-methyl-4-aminopyridinium cation in $\mathbf{4}_2\cdot(Cl_4Q)_3$. Displacement ellipsoids are drawn for the probability of 50 % and hydrogen atoms are shown as spheres of arbitrary radii.

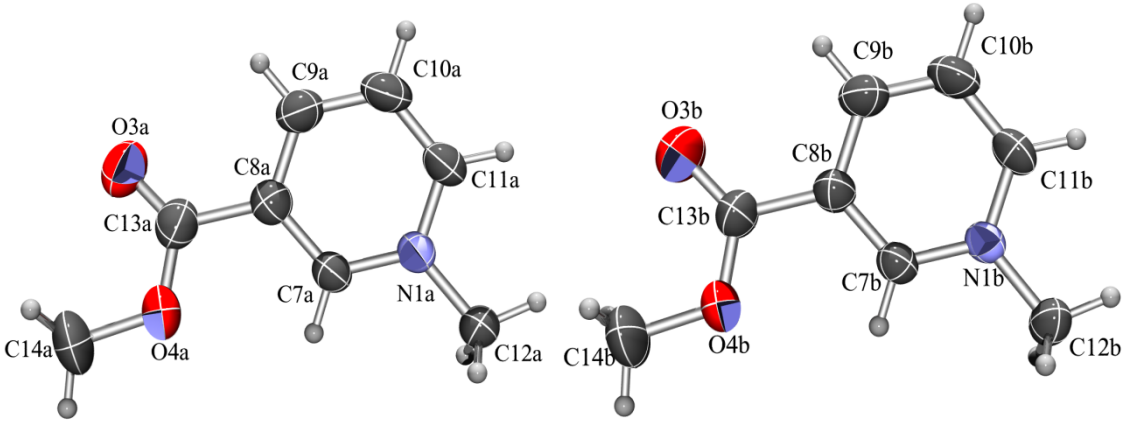

Figure S13 ORTEP-3 drawing of two symmetry-independent *N*-methyl-3-carboxymethylpyridinium cations in $\mathbf{5}_4\cdot(Cl_4Q)_5$. Displacement ellipsoids are drawn for the probability of 50 % and hydrogen atoms are shown as spheres of arbitrary radii.

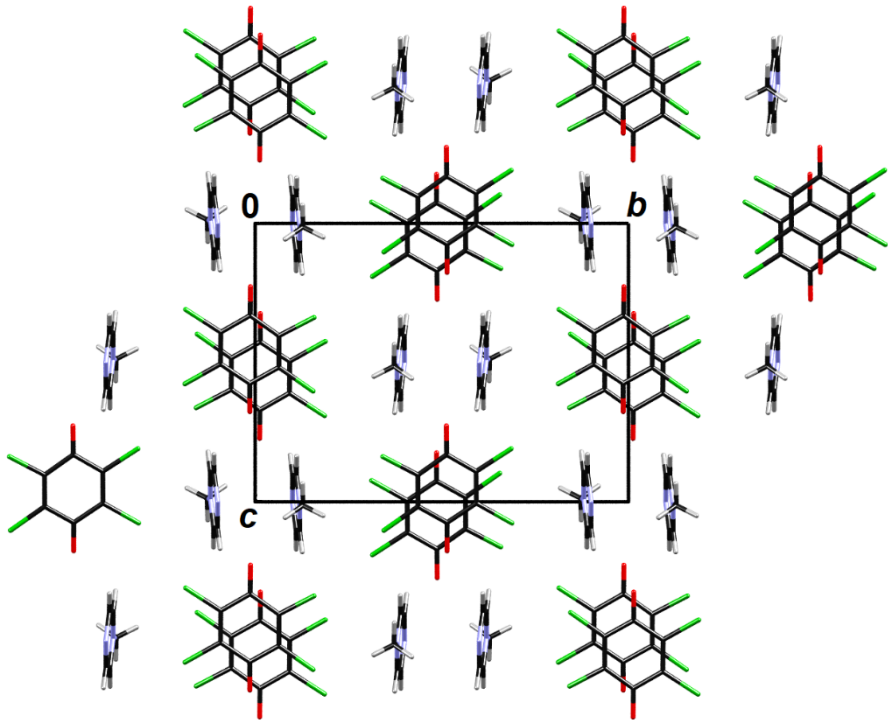

Figure S14 Crystal packing of **1**·Cl_4Q viewed in the direction [100].

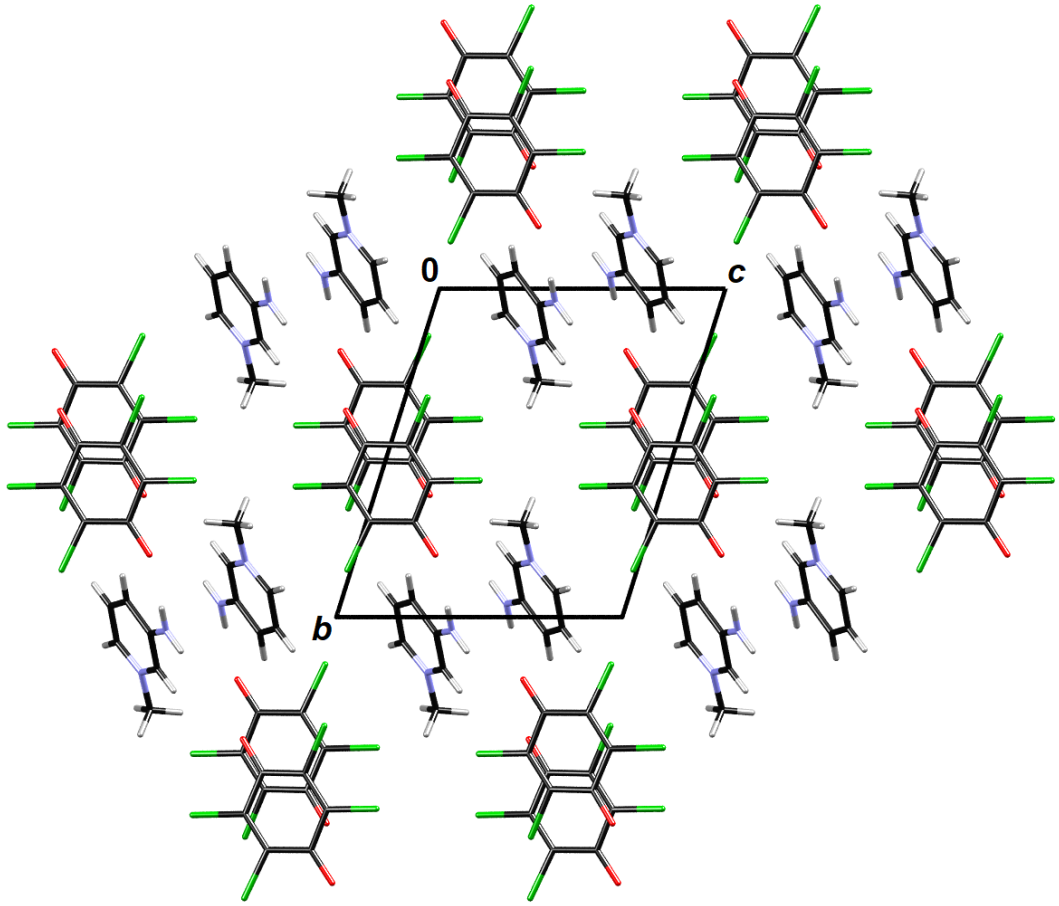

Figure S15 Crystal packing of **3**·Cl_4Q viewed in the direction [100].

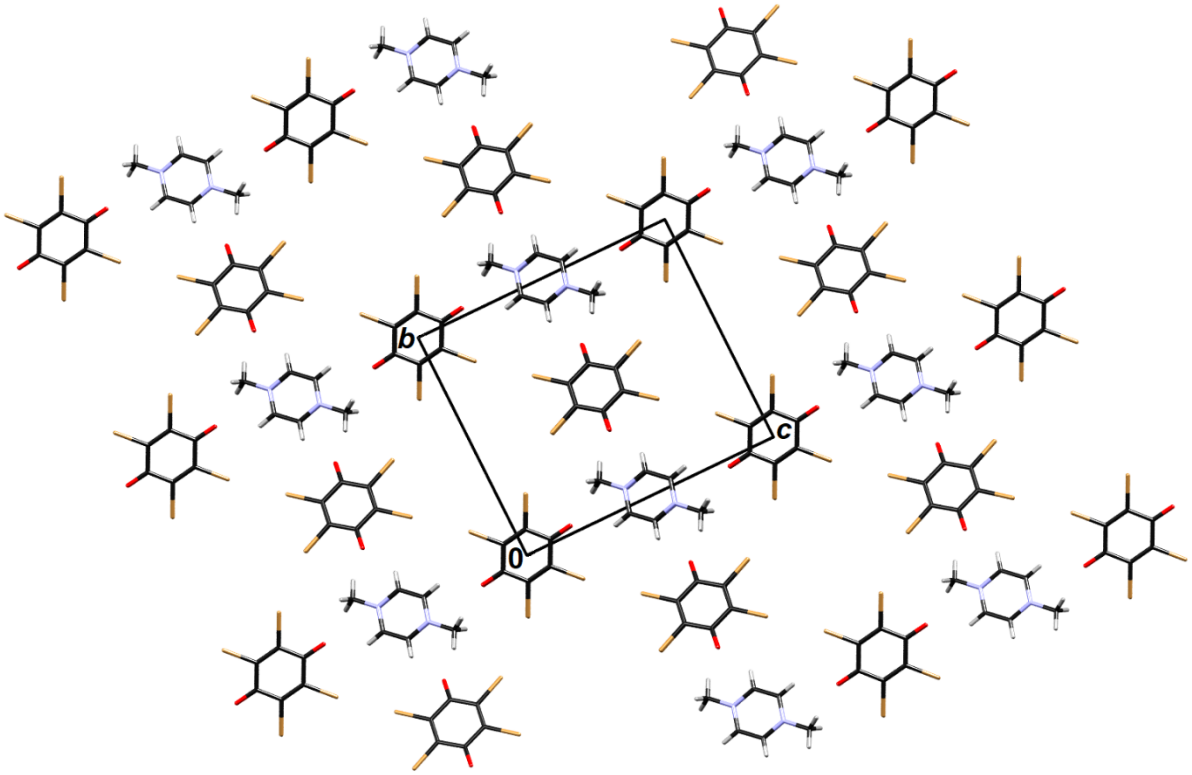

Figure S16 Crystal packing of **4**·$(Br_4Q)_2$ viewed in the direction [100].

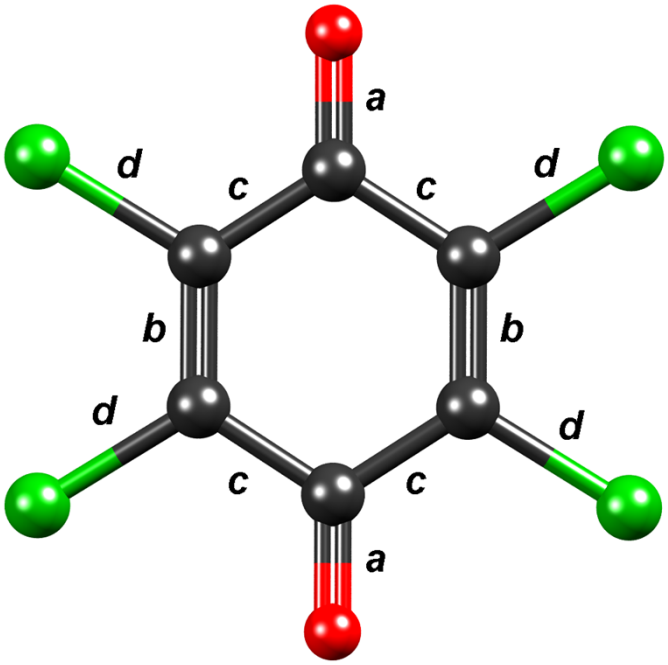

Figure S17 Different types of bonds in the (semi)quinone ring used for geometric correlation between bond lengths and charge of the ring shown in Figs. S18-S21.

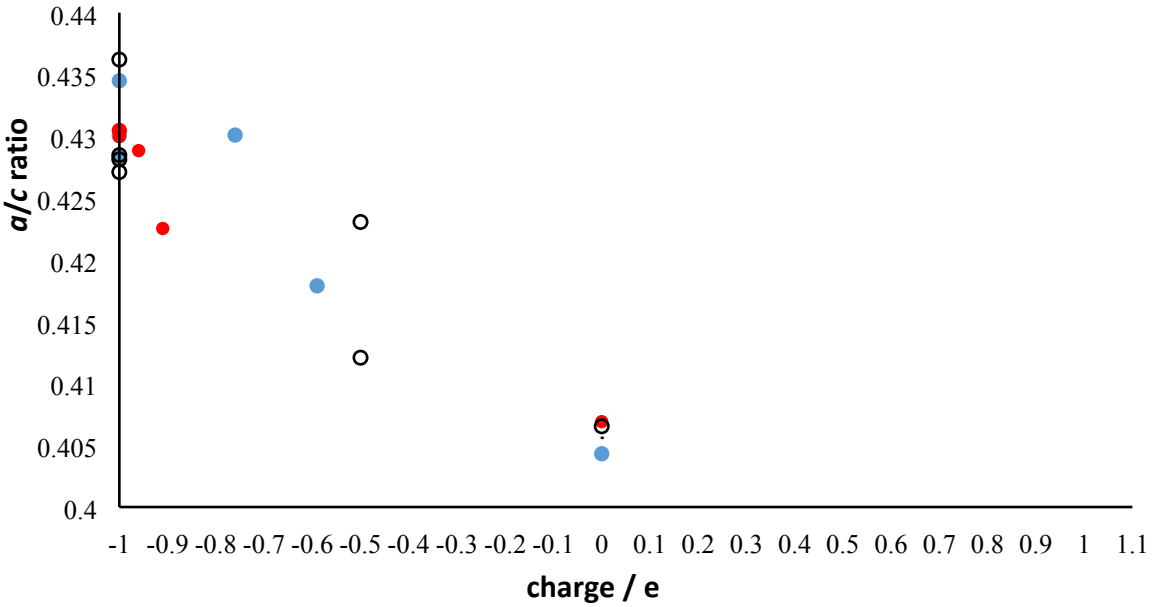

Figure S18 Correlation between bond lengths in the semiquinone radicals and their charges, after Kistenmacher *et al*. [1]: *a*/*c* (definition is given in Fig. S17). Data for Cl_4Q radicals from accurate X-ray charge density studies [2,3] are shown as red full circles; data for for Cl_4Q radicals from this work are shown as blue full circles and data for Br_4Q radicals from this work are shown as empty black circles.

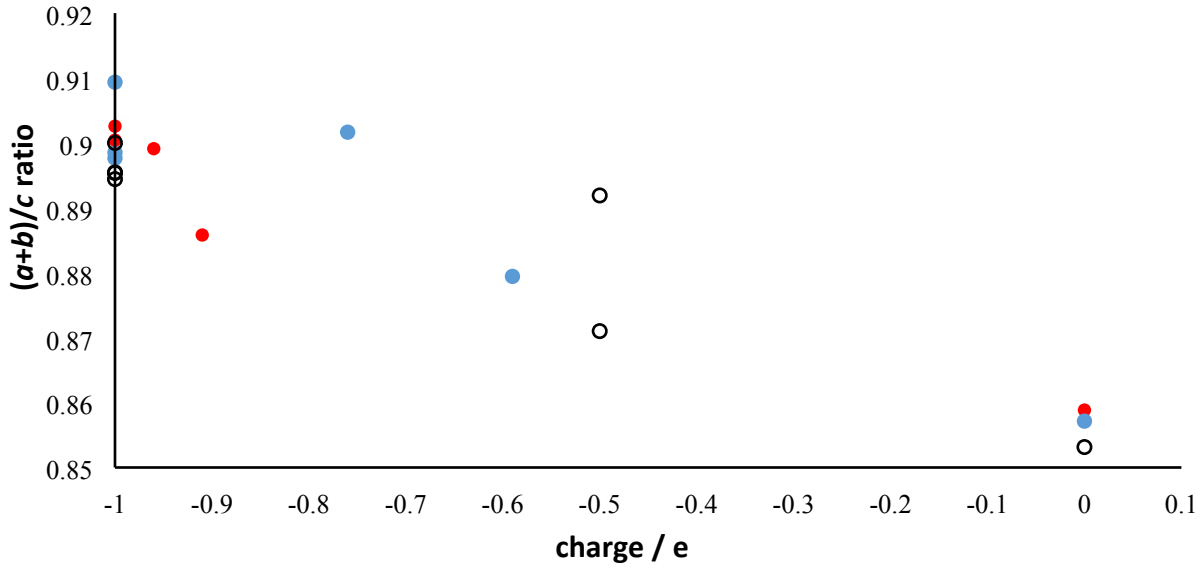

Figure S19 Correlation between bond lengths in the semiquinone radicals and their charges, after Coppens & Guru Row [4]: (*a*+*b*)/*c* (definition is given in Fig. S17). Data for Cl_4Q radicals from accurate X-ray charge density studies [2,3] are shown as red full circles; data for Cl_4Q radicals from this work are shown as blue full circles and data for Br_4Q radicals from this work are shown as empty black circles.

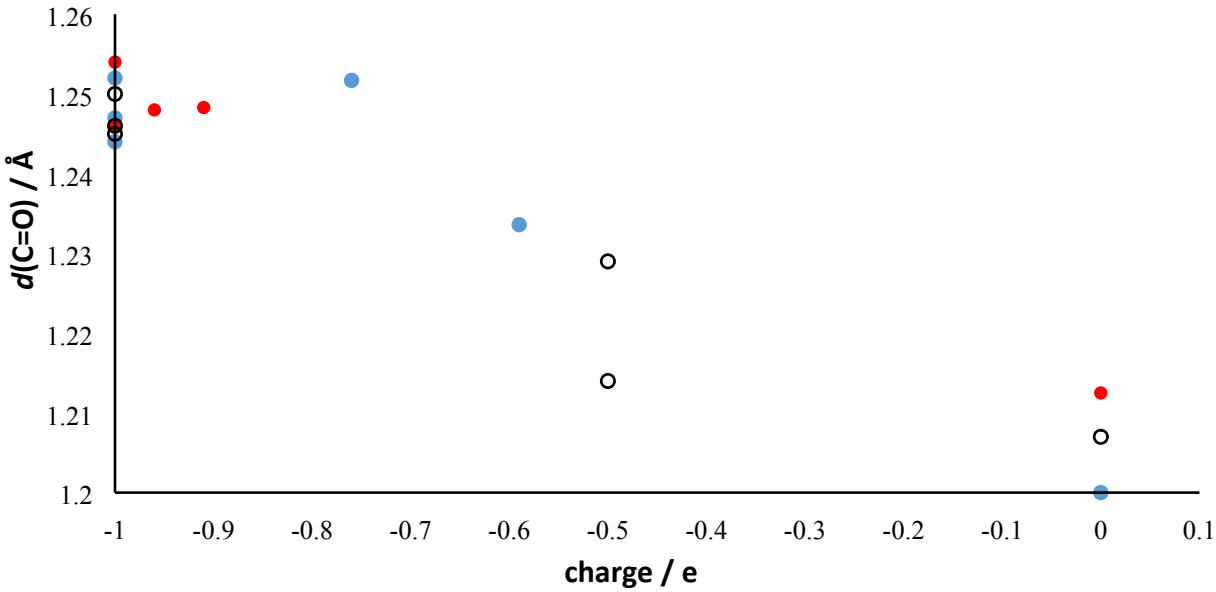

Figure S20 Correlation between C=O (*a* in Fig. S17) bond lengths of the semiquinone radicals and their charges. Data for Cl_4Q radicals from accurate X-ray charge density studies [2,3] are shown as red full circles; data for Cl_4Q radicals from this work are shown as blue full circles and data for Br_4Q radicals from this work are shown as empty black circles.

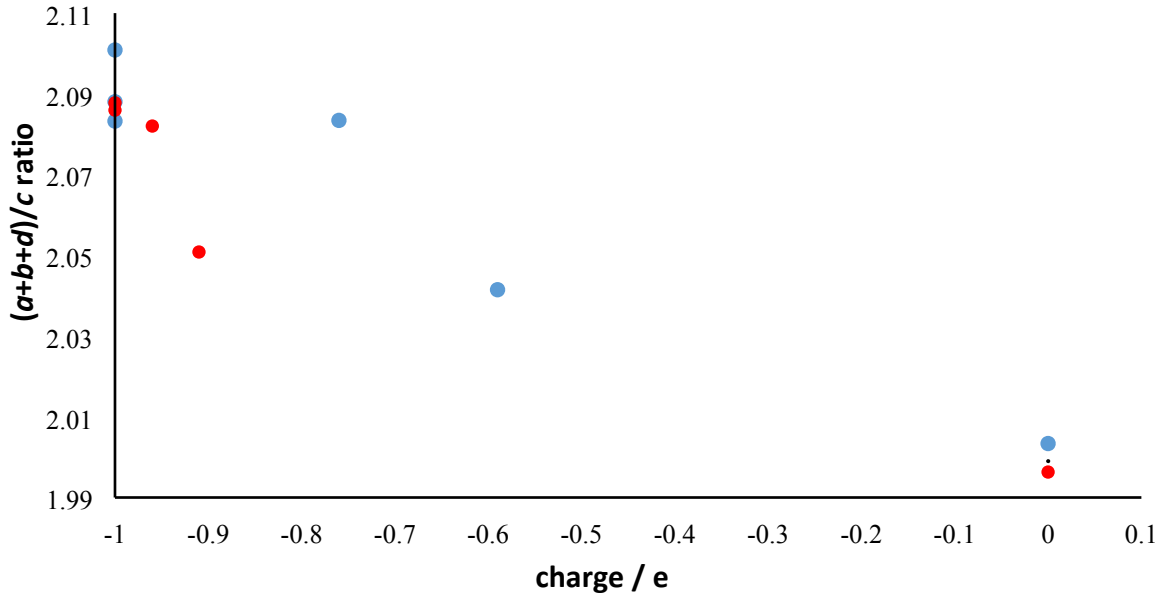

a)

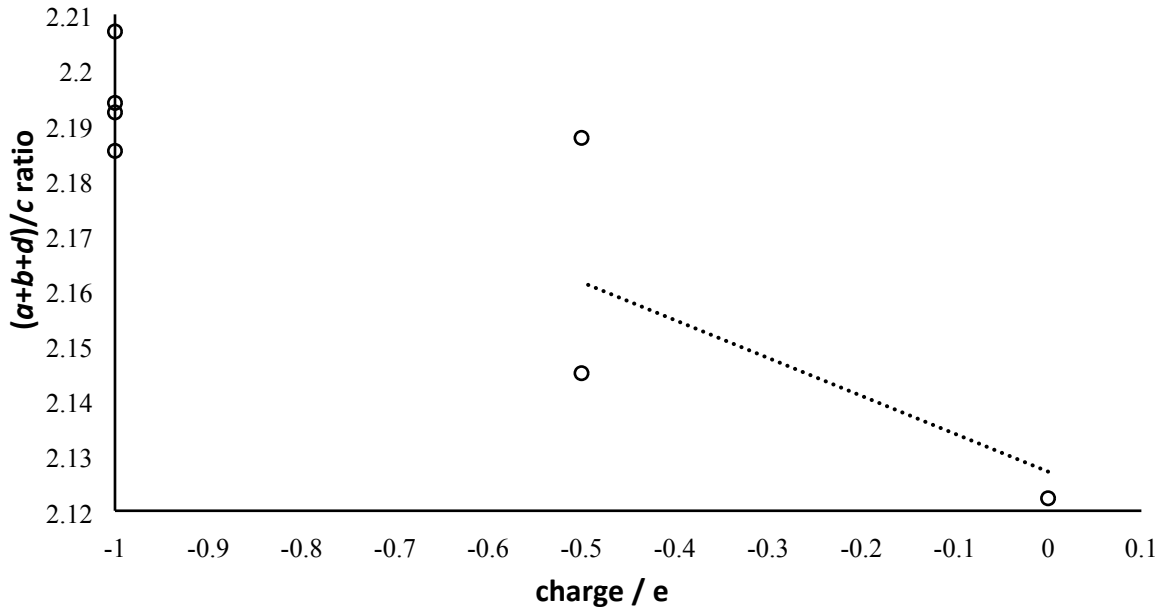

b)

Figure S21 Correlations between bond lengths in the semiquinone radicals and their charges proposed in this work: (*a*+*b*+*d*)/*c* (definition is given in Fig. S17). a) Data for Cl_4Q radicals from accurate X-ray charge density studies [2,3] are shown as red full circles and data for Cl_4Q radicals from this work are shown as blue full circles; b) data for Br_4Q radicals from this work are shown as empty black circles.

References

1 T. J. Kistenmacher, T. J. Emge, A. N. Bloch and D. O. Cowan, *Acta Crystallogr.*, 1982, **38**, 1193−1199.

2 K. Molčanov, C. Jelsch, B. Landeros, J. Hernández-Trujillo, E. Wenger, V. Stilinović and B. Kojić-Prodić, C. Escudero-Adan, *Cryst. Growth Des.*, 2019, **19**, 391-402.

3 K. Molčanov, Z. Mou, M. Kertesz, B. Kojić-Prodić, D. Stalke, S. Demeshko, A. Šantić and V. Stilinović, *Chem. Eur. J.*, 2018, **24**, 8292-8297.

4 P. Coppens and T. N. Guru Row, *Ann. N. Y. Acad. Sci.*, 1978, **313**, 244-255.